# Polycyclic aromatic hydrocarbons in leaves of *Cinnamomum camphora* along the urban–rural gradient of a megacity: Distribution varies in concentration and potential toxicity

Shan Yin [a,b,c,d,*,1], Haoxin Tan [a,b,c,1], Nan Hui [a,b,c,d], Yingge Ma [e,f], Lu Tian [a,b,c], Ningxiao Sun [a,b], Chunjiang Liu [a,b,c,d]

[a] *School of Agriculture and Biology, Shanghai Jiao Tong University, 800 Dongchuan Rd., Shanghai 200240, China*
[b] *Shanghai Urban Forest Ecosystem Research Station, National Forestry and Grassland Administration, 800 Dongchuan Rd., Shanghai 200240, China*
[c] *Yangtze River Delta Ecology & Environmental Change and Control Research Station, Ministry of Education, 800 Dongchuan Rd, Shanghai 200240, China*
[d] *Key Laboratory for Urban Agriculture, Ministry of Agriculture and Rural Affairs, 800 Dongchuan Rd., Shanghai 200240, China*
[e] *Shanghai Academy of Environmental Sciences, 508 Qinzhou Rd., Shanghai 200233, China*
[f] *State of Environmental Protection Key Laboratory of the Formation and Prevention of Urban Air Complex, 508 Qinzhou Rd., Shanghai 200233, China*

## HIGHLIGHTS

- 84 sampling sites along the urban–rural gradient in Shanghai were studied.
- PAH concentration in *C. camphora* leaves decreased along the urban–rural gradient.
- Trend of PAH concentration corresponded to that of population density.
- High PAH potential toxicity in sites resulted from adjacent industrial districts.
- Urban-Suburban-rural junction areas merit more ecological risk attention.

## GRAPHICAL ABSTRACT
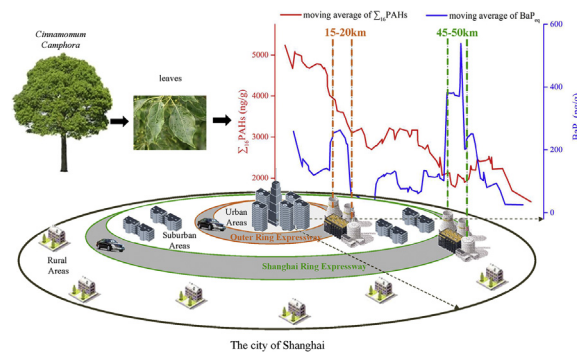


## ARTICLE INFO

## ABSTRACT

Rapid urbanization and industrialization have precipitated the significant urban-rural gradient involving various aspects of human-related activities especially in megacities. Anthropogenic activities are the main source of polycyclic aromatic hydrocarbon (PAH) contamination, and the rising awareness concerning PAH potential toxicity to human health promotes a further understanding of its spatial distribution pattern in cities. Whether the distribution of PAH concentration and potential toxicity respond to the urban-rural gradient still requires investigation. This study applied a grid sampling method to investigate PAH concentration using *Cinnamomum camphora* leaves as bioindicators which were obtained from 84 sampling sites in a megacity, Shanghai. The potential toxicity of PAHs in leaves was calculated by toxicity factor equivalent method. Results revealed the patterns of PAH distribution in the city varied in concentration and potential toxicity: the total concentration of PAHs in leaves decreased along the urban–rural gradient, while the potential toxicity peaked at junction areas. The trend of PAH concentration along the distance from urban center corresponded to that of population density. The spatial distribution of potential toxicity did not correspond with the gradient but was influenced by high benzo(*a*)pyrene concentration originated from

---

* Corresponding author at: School of Agriculture and Biology, Shanghai Jiao Tong University, 800 Dongchuan Rd., Shanghai 200240, China.
  *E-mail address:* yinshan@sjtu.edu.cn (S. Yin).
  [1] These authors have contributed equally to this work.

the industry districts nearby. Higher potential toxicity of PAHs was observed at the urban-suburban-rural junction areas of megacities, advocating health-risk attention and appropriate plan for land use of these transition areas in cities.

## 1. Introduction

Polycyclic aromatic hydrocarbons (PAHs) are a class of organic pollutants distributed ubiquitously in urban environment matrices that have attracted major concern for their mutagenic and carcinogenic properties (Froger et al., 2019; Zhang et al., 2019). In urban environments, people are exposed to PAHs through different ways such as inhalation through air, digestion through water and vegetables grown in soil (Kargar et al., 2017). Repeated contact with PAHs may cause skin inflammation, kidney and liver damage, and even tumors and cancer through cellular membrane function interference and damage (Samburova et al., 2016; Saxena et al., 2014).

Due to the importance of ecological safety in cities, it is critical to measure the accumulations of PAHs and to assess the potential toxicity against human health. Plant leaves serve as appropriate PAHs (especially in atmospheric environment) contamination bioaccumulators and bioindicators. Foliar cuticular lipophilic substances and wax can intercept PAHs mainly through atmospheric deposition (Desalme et al., 2013; Tavera Busso et al., 2018; De Nicola et al., 2014). Hence, the evaluation of the potential toxicity of PAHs in leaves can function as an auxiliary assessment of the airborne PAHs risk. Moreover, the relationship of lymphocytes DNA damage with leaf PAHs contaminations has also been reported (Alabi et al., 2012). Therefore, the assessment of the PAHs toxicity in leaves is necessary. Benzo($a$)pyrene (BaP), recognized as the greatest hazard congener among 16 priority PAHs, is the most studied component of the PAHs family (Roy et al., 2019). In order to express the toxicity of each PAHs with relation to BaP, equivalents of BaP (BaP$_{eq}$) have been used extensively in evaluating potential toxicity associated with PAHs in urban environments and are calculated by multiplying the toxic equivalency factors (TEFs) of each PAH by their concentrations (Jakovljević et al., 2015; Zhang et al., 2019).

The spatial distribution variations of urban space and human-related activity cause some pollutants in various urban environment matrices to exhibit certain distribution characteristics along the urban–rural gradient, such as PM$_{2.5}$, ozone, and several heavy metal ions in urban soil (Li et al., 2019; Xiao et al., 2013; Zhao et al., 2019). PAHs are one of the most common pollutants in urban environments (particularly in the air), and their distribution in various environment matrices may also be affected by urban gradients. Yu et al. (2018) have determined the concentrations of PAHs on organic films on 35 glass surfaces in Shanghai and noted that the concentrations of PAHs on organic films decreased along the urban–rural gradient. Also, previous work has reported that the PAHs values in the leaves of 28 samples of holly in the southern Campania region of Italy were highest in urban sites, followed by suburban sites, and were lowest in remote sites (De Nicola et al., 2017).

The distribution of PAH potential toxicity is typically consistent with that of PAH total concentration because of the significant positive correlation between them in city (Zhang et al., 2019). Therefore, PAH potential toxicity in urban area is generally higher than that in suburban and rural areas. However, some regions in suburban and rural areas often have concentrated pollution sources (industry, traffic, etc.), leading to high potential toxicity of PAHs in the soil, air, and other environment matrices there (Yu et al., 2019). Studies have demonstrated that the potential toxicity of PAHs bounded on particle matter is relatively higher in urban industrial zones (Chen et al., 2019; Jakovljević et al., 2015) hence the potential PAH toxicity of these urban areas cannot be ignored.

Studies of the spatial distribution of PAHs in urban environment matrices along urban–rural gradients have primarily focused on soil and water. Few studies have been conducted on the spatial distribution of PAHs in plant leaves or comprehensively have investigated the urban–rural gradient, particularly in megacities. Shanghai, as a megacity and Alpha+ city, was the study area. The distributions of concentration and potential toxicity of PAHs in C. camphora leaves along an urban–rural gradient in Shanghai were analyzed.

In particular, we tried to answer the following questions:

1. In a typical megacity such as Shanghai, what are the spatial distributions of the concentration and potential toxicity of PAHs in C. camphora leaves?
2. Do the spatial distribution of concentration and potential toxicity of PAHs in C. camphora leaves correspond with the urban–rural gradient?

## 2. Materials and methods

### 2.1. Study area

We studied Shanghai, a megacity with high urbanization level and significant urban–rural gradient. Shanghai is located at the eastern edge of Eurasia bordering the Pacific Ocean with an average altitude of about 4 m and a climate of subtropical monsoon. The city has an area of 6340 km$^2$ and a population of 24.18 million. The sample points were deployed on the basis of an 80 km × 100 km grid containing eighty 10 × 10 squares, with each square center as the sampling point. The grid provided 74 sampling points (6 square centers were located outside Shanghai) including Chongming Island, and 10 more were added in the urban center in order to balance the point number among urban center, suburban and rural areas, yielding a total of 84 sampling points (Fig. 1).

Distance from the urban center was adopted to describe the urban–rural gradient. Many studies on Shanghai's urban–rural gradients have separated Shanghai into three regions according to urbanization level (e.g. Tian et al., 2015; Wang et al., 2017; Yu et al., 2018). Generally, areas inside Outer Ring Expressway (S20) are urban areas, those between the Outer Ring Expressway (S20) and Shanghai Ring Expressway (G1503) are suburban areas, and those outside Shanghai Ring Expressway (G1503) are rural areas. Besides, buffering analysis and an overlay method were applied to divide 84 sites into different distance groups (Fig. 1).

### 2.2. Sample collection

We studied C. camphora, a typical tree species in the Yangtze River Delta and an evergreen broad-leaved tree species widely used in urban forests and green spaces of Shanghai (Yang et al., 2017). Leaves of C. camphora are rich in waxy substances and have been reported to be capable of adsorbing PAHs in air, thus making them effective PAH bioindicators (Tian et al., 2019; Yang et al., 2017). The sampling time started from 3rd May (2018) and all the samplings were collected within 3 days. During the sampling days, the average value of PM$_{2.5}$ was 41 μg/cm$^3$ and the average temperature was 22 °C. Three plots were selected at each site, and samples were collected from three mature and healthy C. camphora trees (10–20 years old) at each plot. Pruning shears were used to remove 5 branches at 3–5 m above the ground from 4 different directions (N, S, E, W) of each tree and
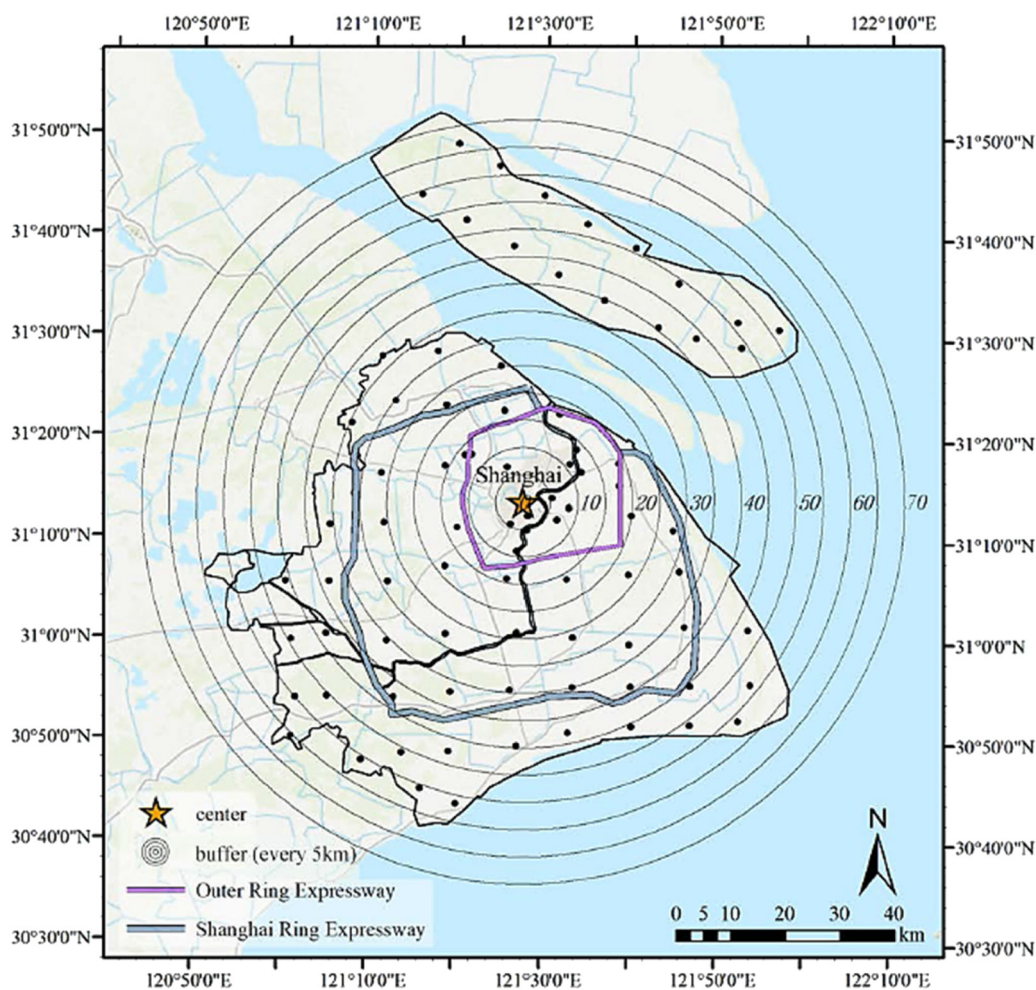
**Fig. 1.** Study area and 84 sampling sites.

approximately 100 pieces of leaves were carefully removed from the branches and mixed into one sample, yielding 252 samples in total. All samples were placed into polyethylene bags and transported to the lab, where all samples were shattered and stored at −18 °C prior to analysis. It should be noted that no samples were rinsed with water.

### 2.3. PAH extraction, purification, and analysis

The 16 priority PAHs listed by US Environmental Protection Agency (2014) were detected and measured as in Tian et al. (2019), and the process was divided into three steps: extraction, purification and enrichment, and quantification.

We used supercritical fluid extraction technology (Spe-ed SPE-15000, USA) for extraction, where three to four extractions were set for each sample and each extraction contained 5-g leaf samples. The extraction comprised two stages. The first was a 15-min static extraction with a pressure of 350 atm and an oven temperature of 180 °C. The second was a 30-min dynamic extraction, where the temperature was reduced to 110 °C. The silica–alumina columns (CNWBOND 800 mg silica/1200 mg Alumina SPE Cartridge, 2 g, 6 mL) were used to purify the extracted samples through solid-phase extraction. The PAH elution was finally concentrated to 0.5 mL, which will be analyzed through gas chromatography–mass spectrometry (GC/MS, Agilent 7890 A/5977 A) with parameter set as conducted in previous work (Fellet et al., 2016). Briefly, the oven temperature program started at 55 °C then was shifted to 200 °C at 25 °C/min, to 320 °C at 10 °C/min and to 325 °C at 25 °C/min, with a final isothermal stage lasting for

10 min. We took the average concentration of the 3 plots as the PAH concentration of each site.

### 2.4. Quality control and quality assurance

Quality assurance and quality control were conducted with one spike blank and one procedural blank for every 7 samples. Based on each PAH, the detection limit for the analytical procedure ranged from 0.005 to 0.022 ng/g. The target compounds were below the limit of detection in the procedural blank. The average recovery of the 16 PAHs ranged from 82% to 120% and PAH concentrations were corrected by the recovery percentages. The relative standard deviations of the duplicate samples were below 20%.

**Table 1**
TEFs of 16 PAHs.

| TEF | Rings | PAH |
|---|---|---|
| 1 | 5 | Benzo[a]pyrene Dibenz[a,h]anthracene |
| | 4 | Benz[a]anthracene |
| 0.1 | 5 | Benzo[b]fluoranthene Benzo[j + k]fluoranthene |
| | 6 | Indeno[1,2,3-cd]pyrene |
| | 3 | Anthracene |
| 0.01 | 4 | Chrysene |
| | 6 | Benzo[g,h,i]perylene |
| | 2 | Naphthalene |
| 0.001 | 3 | Acenaphthylene Acenaphthene Fluorene Phenanthrene |
| | 4 | Fluoranthene Pyrene |

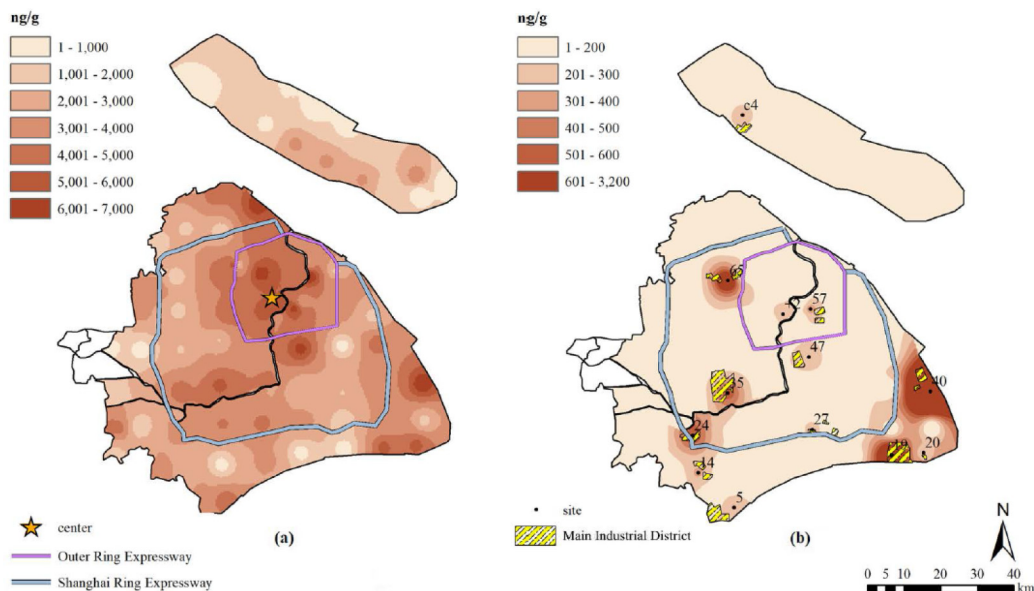**Fig. 2.** Spatial distributions of $\Sigma_{16}$PAHs and BaP$_{eq}$ in *C. camphora* leaves in Shanghai. (a) $\Sigma_{16}$PAHs; (b) BaP$_{eq}$.

## 2.5. Methods for potential toxicity assessment

Potential toxicities of 16 PAHs in *C. camphora* leaves were quantified with BaP$_{eq,}$ on the basis of TEFs. BaP$_{eq}$ of the total concentration was measured as follows:

$$BaP_{eq} = \sum_{i=1}^{n} MEC_i \times TEF_i \tag{1}$$

where $MEC_i$ (ng/g) represented the concentration of PAHs in leaves of *C. camphora* and $TEF_i$ represented the toxic equivalency factor. The TEFs were adopted from research by De Nicola et al. (2014) and are listed in Table 1.

## 2.6. Statistical analysis

To quantify the intensity of anthropogenic activities, local population density (PD) was calculated by dividing the number of people residing in registered households by the area of sub administrative units of the 84 sites; these values were obtained by consulting statistical data (2018) of the almanac and its official statistical network of each district. The population density of the 84 sample points included Shanghai's 13 administrative districts and 65 sub administrative units in total.

Pearson correlation for calculating correlations between PAHs data and the parameters was applied using SPSS24.0 (IBM, USA). The moving values (Fig. 4) were obtained through a smoothing method in Origin 9.1

(OriginLab, USA). The distribution of total PAH concentrations and BaP$_{eq}$ in Shanghai (Fig. 2) was visualized using the interpolation of the inverse distance weight method in ArcMap 10.2 (ESRI, USA).

## 3. Results and discussion

### 3.1. Distribution patterns of PAH concentration and potential toxicity

The concentrations of PAHs in the *C. camphora* leaves were shown in PAHs concentration data.xlsx. The total concentrations of 16 PAHs ($\Sigma_{16}$PAHs) ranged from 188.1 to 6997 ng/g, with an average value of 3014 ng/g. The average $\Sigma_{16}$PAHs at urban, suburban, and rural areas, were 4670.7, 3365.1, 2338.9 ng/g, respectively. BaP$_{eq}$ of $\Sigma_{16}$PAHs in *C. camphora* leaves ranged from 3.9 to 3134.7 ng/g, with an average value of 159.9 ng/g. The averages of BaP$_{eq}$ (ng/g) were: urban, 131.2; suburban, 164.5; rural, 164.8. $\Sigma_{16}$PAHs showed a clearly decrease along the urban-suburban-rural transect (Fig. 2a) whereas BaP$_{eq}$ only reached high levels in some suburban and rural areas (Fig. 2b). $\Sigma_{16}$PAHs decreased linearly (p < .001) along the distance from urban center (Fig. 3), which indicated that $\Sigma_{16}$PAHs in *C. camphora* leaves responded to the urban–rural gradient. No significant correlation between BaP$_{eq}$ and distance from urban center was found.

Although the Pearson correlation analysis indicated a strong positive correlation (0.402, p < .001) between BaP$_{eq}$ and $\Sigma_{16}$PAHs, the distribution patterns of them varied significantly along the urban-rural gradient. The potential toxicities at some sites in suburban and rural areas were actually higher than those in urban areas which had higher
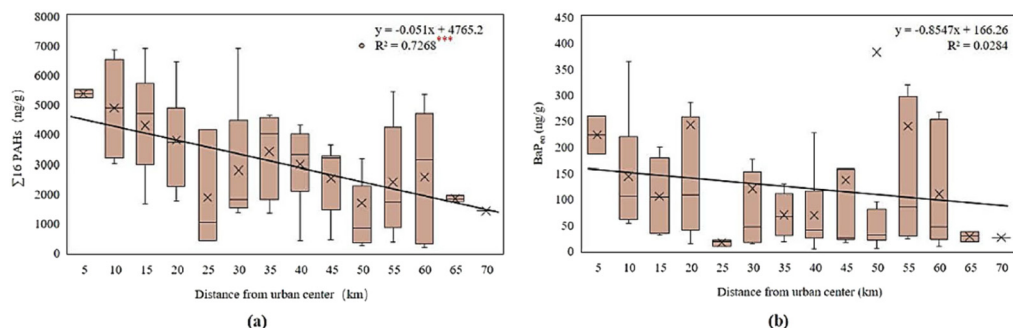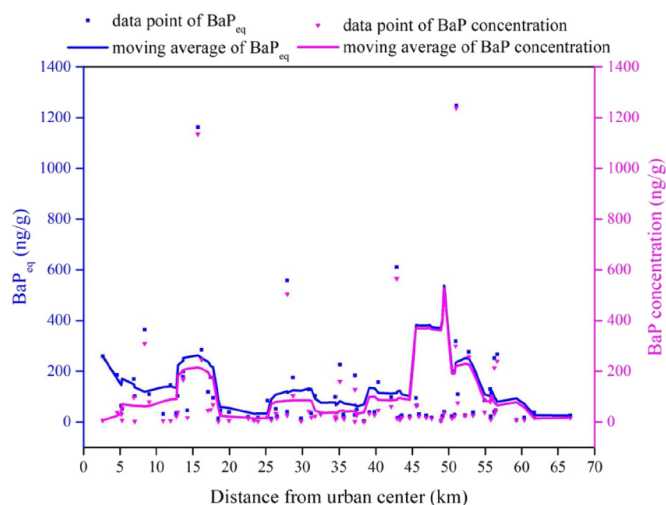


**Fig. 3.** $\Sigma_{16}$PAHs and BaP$_{eq}$ in *C. camphora* leaves along the distance from urban center. (a) $\Sigma_{16}$PAHs; (b) BaP$_{eq}$. ***: p < .001.

**Fig. 4.** Mean values of BaP$_{eq}$ and BaP concentrations in *C. camphora* leaves along the urban–rural gradient of Shanghai.



**Fig. 6.** Mean values of population density, $\Sigma_{16}$PAHs and BaP$_{eq}$ in *C. camphora* leaves along the urban–rural gradient of Shanghai.
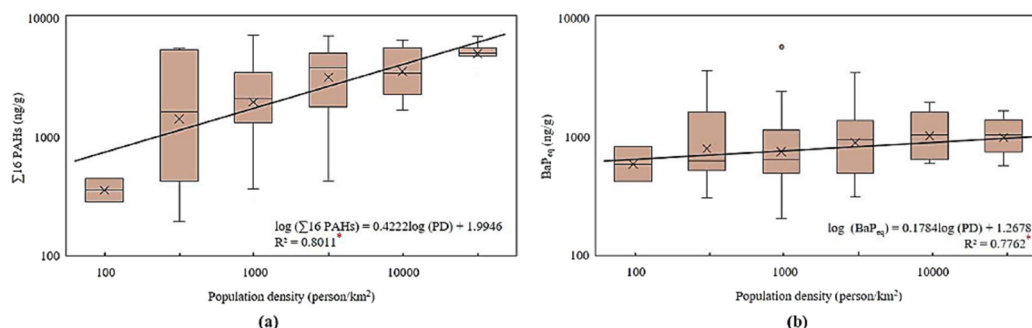
concentrations. We attributed the seemingly conflicting results to different spatial distribution of BaP and other PAHs obtained in our study (see PAHs concentration data.xlsx) and their quite different contribution to BaP$_{eq}$. The relationship between the BaP concentrations and BaP$_{eq}$ will be discussed below.
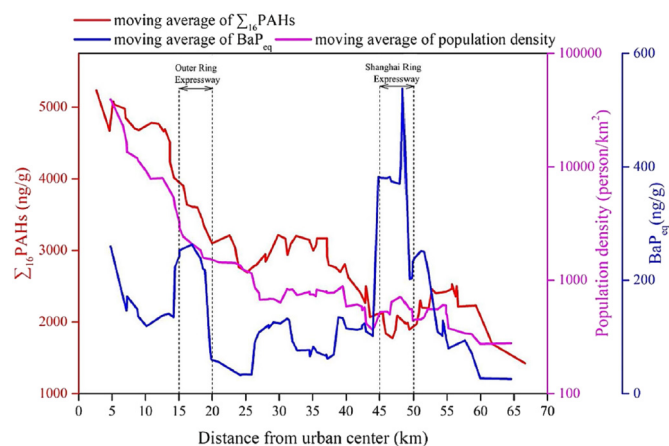
### 3.2. BaP concentration and BaP$_{eq}$

Fig. 4 shows that BaP$_{eq}$ was mainly determined by the concentration of BaP due to its 10–1000 fold higher TEF (TEF = 1) than other PAHs (TEF = 0.001–0.1, Table 1). Except for the 5-km distance between the two groups, their values and changing trends nearly coincided (Fig. 4), which indicated that the spatial distribution of the potential toxicity of PAHs in *C. camphora* leaves did not respond to the urban–rural gradient but were mainly affected by the measured concentrations of BaP. BaP mainly originates from industry and traffic sources (combustion of coal, diesel, and gasoline) (Bieser et al., 2012; Hanedar et al., 2014; Jakovljević et al., 2015). Therefore, we should focus on the vicinities of industrial areas and high-density roads which may bare higher potential toxicity.

### 3.3. Relationship of $\Sigma_{16}$PAHs and BaP$_{eq}$ with population density along the urban-rural gradient

Both $\Sigma_{16}$PAHs and BaP$_{eq}$ had a strong positive correlation with local population density (Fig. 5), with the Pearson r of 0.895 and 0.881, and therefore strongly indicates anthropogenic PAHs source such as cooking, heating, smoking and vehicle emissions as principle PAHs sources. The regression equation (Fig. 5a) was consistent with that in

the study conducted by Sharma et al. (2018), in which the regression slope of the log-transformed population versus the air concentration of $\Sigma$PAHs was 0.609. Slopes approaching 0.5 suggested that a 10-fold increase in population might lead to a 10% increase in PAH concentration, which was also consistent with two other studies (Hafner et al., 2005; Wang et al., 2010). In addition, the similar trend of population density versus PAH concentration in leaves of *C. camphora* and in air may further support the validity of the *C. camphora* as a bioindicator of PAHs in atmospheric environment.

Fig. 6 visualizes the spatial variance of $\Sigma_{16}$PAHs, BaP$_{eq}$ and local population density along the distance. The trend curves of $\Sigma_{16}$PAHs and local population density along the distance coincide and thus further supports $\Sigma_{16}$PAHs was mainly influenced by the level of population-related PAHs emissions (Fig. 6). Both $\Sigma_{16}$PAHs and local population density decreased rapidly at sites <20 km from the city center and showed less sharp decrease at sites exceeding 20 km. Therefore, we attributed the distribution of $\Sigma_{16}$PAHs along the urban-rural gradient to the intensity of the population-related source.

### 3.4. PAH diagnostic ratios

PAH diagnostic ratios have been widely applied in biomonitoring studies to identify pollution source of PAHs, such as fluoranthene/ (fluoranthene + pyrene) [Fla/(Fla + Pyr)], indeno[1,2,3-c,d]pyrene/ (indeno[1,2,3-c,d]pyrene + benzo[g,h,i]perylene) [InP/(InP + B[ghi] P)] (De Nicola et al., 2014; Tobiszewski and Namiesnik, 2012). Values for [Fla/(Fla + Pyr)] below 0.4 and for InP/(InP + B[ghi]P) below 0.20 indicate petroleum input; values for Fla./(Fla + Pyr) from 0.40 to 0.50 and InP/(InP + B[ghi]P) from 0.20 to 0.50 are indicative of liquid fuel oil combustion; and those for Fla./(Fla + Pyr) and InP/



**Fig. 5.** Correlation between $\Sigma_{16}$PAHs and BaP$_{eq}$ with local population density (PD.). (a) $\Sigma_{16}$PAHs; (b) BaP$_{eq}$. *: p < .05.

**Table 2**
Diagnostic ratios for PAHs in bioindicators in different studies.

| Reference | Location | Bioindicator | Min–max(Median) | |
|---|---|---|---|---|
| | | | Fla/(Fla + Pyr) | InP/(InP + B[*ghi*]P) |
| Our study | Shanghai | *Cinnamomum camphora* | 0.13–0.99(0.86) | 0.01–0.66(0.12) |
| De Nicola et al., 2014 | Urban area in Naples, Italy | *Quercus ilex* | 0.32–0.60(0.45) | n.c.–1.00(0.39) |
| De Nicola et al., 2014 | Remote area in Naples, Italy | *Quercus ilex* | 0.48–1.00(0.62) | 0.26–1(0.59) |
| Kargar et al., 2017 | Aliaga industrial district of Izmir | *Pine* | 0.65–0.95(n.c.) | 0.1–0.5(n.c.) |
| Rotaru et al., 2017 | Urban areas in Romania | Moss | 0.35–0.75(0.55) | n.c. |

n.c.: not calculable.

(InP + B[*ghi*]P) > 0.50 suggest coal, grass or solid fuel combustion (Kargar et al., 2017; Fasani et al., 2016).

PAH diagnostic ratios for Fla./(Fla + Pyr) and InP/(InP + B[*ghi*]P) were calculated and compared with other literature (Table 2). In our study, 92% Fla./(Fla + Pyr) values were above 0.5, whereas 64% InP/(InP + B[*ghi*]P) values were below 0.2 and 30% ranged from 0.2 to 0.5. The ratios were indicative of mixed petroleum and fuel combustion sources which is consistent with previous work of De Nicola et al. (2011). While the diagnostic ratios are proved to be effective in studies of other environmental matrices, its effect in bioindicator studies need further investigation. The diagnostic ratios can provide good indication when the sources are limited, but it can be difficult in areas like megacities where the sources of airborne PAHs are complex (De Nicola et al., 2014). In addition, degradation, uptake mechanism and photoreaction that occur on bioindicators can modify the PAHs concentration patterns, thus changing the ratios (De Nicola et al., 2014; Tobiszewski and Namiesnik, 2012).

### 3.5. Distribution of potential toxicity along the urban-rural gradient

#### 3.5.1. High BaP$_{eq}$ level sites were adjacent to industrial districts

As alluded to earlier, the potential toxicity of PAHs demonstrated no obvious urban–rural pattern along the distance but showed high level in some sites. Pearson correlation analysis showed that correlation between the potential toxicity and local population density was not significant. Surprisingly, we found that most sites which reached high BaP$_{eq}$ level of >200 ng/g were adjacent to the large industrial districts of Shanghai. Locations of these sites and adjacent industrial districts were summarized in Table S1 and Fig. 1b. The concentration of BaP accounts for over 85% of BaP$_{eq}$ in most sites, except for site "+2" where the high BaP$_{eq}$ level may result from the highest population density of all sites (39,393 people per km$^2$, Table 2). Hence, the distribution pattern of the potential toxicity was mainly determined by the industrial districts that generated high level of BaP.

#### 3.5.2. Junction areas had higher potential toxicity

In Fig. 6, peaks of potential toxicity were found at sites of 15–20 km and 45–50 km from city center, which are also the range of Outer Ring Expressway (S20) and Shanghai Ring Expressway (G1503). Expressway development is a crucial feature of urban expansion in China and is often the basis for separating urban, suburban, and rural areas (Wang et al., 2019b) and areas around the expressway make up the junction areas. With the process of urban sprawl, junction areas have become ideal site of the industrial districts for low land rent and convenient transportation of expressways and thus lead to higher PAHs contamination. Peng et al. (2016) observed two PAHs peak levels in soil, Beijing, at the distances of 13 km (The 5th Ring Road) and 26 km (The 6th Ring Road) and attributed it to concentrated industrial plants in the junction areas. In addition, heavy traffic on the expressways may also lead to higher toxicity level of PAHs in the junction areas.

Urban–rural integration involves the transition zones. Compared with the centers of urban, suburban, and rural areas, which mainly have commercial, residential, cultural, and educational uses, transition zones primarily involve industrial activity, transportation, and agricultural production (Charlesworth et al., 2011). However, recent industrialization and subsequent urban development have caused negative influences on the environment in junction areas (Lopez-Goyburu and Garcia-Montero, 2018). Distribution of the sites with high BaP$_{eq}$ in *C. camphora* leaves in our study also supported this fact. Except for PAH, other pollutants, e.g. potentially toxic elements, also exhibited increasing levels (Keshavarzi et al., 2019). Besides, junction areas often serve as a base of food for urban areas, a region for water purification and conservation, and a source of urban living and production materials (Kroll et al., 2012). Therefore, the potential toxicity of pollutants in the junction areas, particularly in megacities, merits more attention. This paper may help land managers find an appropriate strategy for land use in response to urbanization in order to enhance environmental security in junction areas.

### 4. Conclusions

Total concentrations of 16 PAHs in Shanghai significantly corresponded to the urban–rural gradient and decreased as the distance from the city center increased. The trend curves of concentration and local population density along the distance coincided, suggesting that the variation in PAH levels was mainly determined by the intensity of human activity. Besides, the similar relationship of population density versus PAH concentration in leaves of *C. camphora* and in air may further support the validity of the *C. camphora* as a bioindicator of airborne PAHs. By contrast, the spatial distribution of the potential toxicity of PAHs in *C. camphora* leaves in Shanghai did not correspond with the urban–rural gradient but were mainly affected by the high emissions of BaP by industrial districts nearby. Numerous industrial areas are often concentrated in urban-rural junction areas, resulting in higher potential toxicity of PAHs. Therefore, these junction areas in megacity deserve more attentions and urban planning should be optimized to implement appropriate land use to ensure environmental security in these areas.

Supplementary data to this article can be found online at https://doi.org/10.1016/j.scitotenv.2020.139328.

### CRediT authorship contribution statement

**Shan Yin:** Conceptualization, Methodology, Writing - original draft, Project administration. **Haoxin Tan:** Methodology, Investigation, Formal analysis. **Nan Hui:** Investigation, Writing - review & editing. **Yingge Ma:** Investigation, Resources. **Lu Tian:** Investigation, Data curation. **Ningxiao Sun:** Resources. **Chunjiang Liu:** Writing - review & editing.

### Declaration of competing interest

The authors declare that they have no known competing financial interests or personal relationships that could have appeared to influence the work reported in this paper.

## Acknowledgements

## References

Alabi, O., Bakare, A., Xu, X., Li, B., Zhang, Y., Huo, X., 2012. Comparative evaluation of environmental contamination and DNA damage induced by electronic-waste in Nigeria and China. Sci. Total Environ. 423, 62–72. https://doi.org/10.1016/j.scitotenv.2012.01.056.

Bieser, J., Aulinger, A., Matthias, V., Quante, M., 2012. Impact of emission reductions between 1980 and 2020 on atmospheric benzo a pyrene concentrations over Europe. Water Air Soil Pollut. 223 (3), 1393–1414. https://doi.org/10.1007/s11270-011-0953-z.

Charlesworth, S., De Miguel, E., Ordóñez, A., 2011. A review of the distribution of particulate trace elements in urban terrestrial environments and its application to considerations of risk. Environ. Geochem. Health 33 (2), 103–123. https://doi.org/10.1007/s10653-010-9325-7.

Chen, Q., Chen, Y., Luo, X.S., Hong, Y.W., Hong, Z.Y., Zhao, Z., Chen, J.S., 2019. Seasonal characteristics and health risks of PM2.5-bound organic pollutants in industrial and urban areas of a China megacity. J. Environ. Manag. 245, 273–281. https://doi.org/10.1016/j.jenvman.2019.05.061.

De Nicola, F., Claudia, L., MariaVittoria, P., Giulia, M., Anna, A., 2011. Biomonitoring of PAHs by using Quercus ilex leaves: Source diagnostic and toxicity assessment. Atmos. Environ. 45 (7), 1428–1433. https://doi.org/10.1016/j.atmosenv.2010.12.022.

De Nicola, F., Alfani, A., Maisto, G., 2014. Polycyclic aromatic hydrocarbon contamination in an urban area assessed by Quercus ilex leaves and soil. Environ. Sci. Pollut. Res. 21 (12), 7616–7623. https://doi.org/10.1007/s11356-014-2665-6.

De Nicola, F., Baldantoni, D., Maisto, G., Alfani, A., 2017. Heavy metal and polycyclic aromatic hydrocarbon concentrations in Quercus ilex L. leaves fit an a priori subdivision in site typologies based on human management. Environ. Sci. Pollut. Res. 24 (13), 11911–11918. https://doi.org/10.1007/s11356-015-5890-8.

Desalme, D., Binet, P., Chiapusio, G., 2013. Challenges in tracing the fate and effects of atmospheric polycyclic aromatic hydrocarbon deposition in vascular plants. Environ. Sci. Technol. 47 (9), 3967–3981. https://doi.org/10.1021/es304964b.

Fasani, D., Fermo, P., Barroso, P.J., Martin, J., Santos, J.L., Aparicio, I., Alonso, E., 2016. Analytical method for biomonitoring of PAH using leaves of bitter orange trees (Citrus aurantium): a case study in South Spain. Water Air Soil Pollut. 227 (10), 11. https://doi.org/10.1007/s11270-016-3056-z.

Fellet, G., Pošćić, F., Licen, S., Marchiol, L., Musetti, R., Tolloi, A., Barbieri, P., Zerbi, G., 2016. PAHs accumulation on leaves of six evergreen urban shrubs: a field experiment. Atmospheric Pollution Research 7 (5), 915–924. https://doi.org/10.1016/j.apr.2016.05.007.

Froger, C., Quantin, C., Gasperi, J., Caupos, E., Monvoisin, G., Evrard, O., Ayrault, S., 2019. Impact of urban pressure on the spatial and temporal dynamics of PAH fluxes in an urban tributary of the Seine River (France). Chemosphere 219, 1002–1013. https://doi.org/10.1016/j.chemosphere.2018.12.088.

Hafner, W.D., Carlson, D.L., Hites, R.A., 2005. Influence of local human population on atmospheric polycyclic aromatic hydrocarbon concentrations. Environ. Sci. Technol. 39 (19), 7374–7379. https://doi.org/10.1021/es0508673.

Hanedar, A., Alp, K., Kaynak, B., Avsar, E., 2014. Toxicity evaluation and source apportionment of polycyclic aromatic hydrocarbons (PAHs) at three stations in Istanbul, Turkey. Sci. Total Environ. 488, 439–448. https://doi.org/10.1016/j.scitotenv.2013.11.123.

Jakovljević, I., Pehnec, G., Vadjić, V., Šišović, A., Davila, S., Bešlić, I., 2015. Carcinogenic activity of polycyclic aromatic hydrocarbons bounded on particle fraction. Environ. Sci. Pollut. Res. 22 (20), 15931–15940. https://doi.org/10.1007/s11356-015-4777-z.

Kargar, N., Matin, G., Matin, A.A., Buyukisik, H.B., 2017. Biomonitoring, status and source risk assessment of polycyclic aromatic hydrocarbons (PAHs) using honeybees, pine tree leaves, and propolis. Chemosphere 186, 140. https://doi.org/10.1016/j.chemosphere.2017.07.127.

Keshavarzi, B., Najmeddin, A., Moore, F., Moghaddam, P.A., 2019. Risk-based assessment of soil pollution by potentially toxic elements in the industrialized urban and peri-urban areas of Ahvaz metropolis, southwest of Iran. Ecotoxicol. Environ. Saf. 167, 365–375. https://doi.org/10.1016/j.ecoenv.2018.10.041.

Kroll, F., Muller, F., Haase, D., Fohrer, N., 2012. Rural-urban gradient analysis of ecosystem services supply and demand dynamics. Land Use Policy 29 (3), 521–535. https://doi.org/10.1016/j.landusepol.2011.07.008.

Li, S.J., Yang, L., Chen, L.D., Zhao, F.K., Sun, L., 2019. Spatial distribution of heavy metal concentrations in peri-urban soils in eastern China. Environ. Sci. Pollut. Res. 26 (2), 1615–1627. https://doi.org/10.1007/s11356-018-3691-6.

Lopez-Goyburu, P., Garcia-Montero, L.G., 2018. The urban-rural interface as an area with characteristics of its own in urban planning: a review. Sustain. Cities Soc. 43, 157–165. https://doi.org/10.1016/j.scs.2018.07.010.

Peng, C., Wang, M.I., Chen, W.P., 2016. Spatial analysis of PAHs in soils along an urban-suburban-rural gradient: scale effect, distribution patterns, diffusion and influencing factors. Sci. Rep. 6, 10. https://doi.org/10.1038/srep37185.

Ratola, N., Alves, A., Lacorte, S., Barcelo, D., 2012. Distribution and sources of PAHs using three pine species along the Ebro River. Environ. Monit. and Assess. 184 (2), 985–999. https://doi.org/10.1007/s10661-011-2014-x.

Roy, R., Jan, R., Gunjal, G., Bhor, R., Pai, K., Satsangi, P.G., 2019. Particulate matter bound polycyclic aromatic hydrocarbons: toxicity and health risk assessment of exposed inhabitants. Atmos. Environ. 210, 47–57. https://doi.org/10.1016/j.atmosenv.2019.04.034.

Samburova, V., Connolly, J., Gyawali, M., Yatavelli, R.L.N., Watts, A.C., Chakrabarty, R.K., ... Khlystov, A., 2016. Polycyclic aromatic hydrocarbons in biomass-burning emissions and their contribution to light absorption and aerosol toxicity. Science of the Total Environment 568, 391–401. https://doi.org/10.1016/j.scitotenv.2016.06.026.

Saxena, M., Singh, D.P., Saud, T., Gadi, R., Singh, S., Sharma, S.K., Mandal, T.K., 2014. Study on particulate polycyclic aromatic hydrocarbons over Bay of Bengal in winter season. Atmos. Res. 145–146, 205–213. https://doi.org/10.1016/j.atmosres.2014.04.001.

Sharma, B.M., Melymuk, L., Bharat, G.K., Pribylova, P., Sanka, O., Klanova, J., Nizzetto, L., 2018. Spatial gradients of polycyclic aromatic hydrocarbons (PAHs) in air, atmospheric deposition, and surface water of the Ganges River basin. Sci. Total Environ. 627, 1495–1504. https://doi.org/10.1016/j.scitotenv.2018.01.262.

Tavera Busso, I., Tames, F., Silva, J.A., Ramos, S., Homem, V., Ratola, N., Carreras, H., 2018. Biomonitoring levels and trends of PAHs and synthetic musks associated with land use in urban environments. Sci. Total Environ. 618, 93–100. https://doi.org/10.1016/j.scitotenv.2017.10.295.

Tian, Z.H., Song, K., Da, L.J., 2015. Distribution patterns and traits of weed communities along an urban-rural gradient under rapid urbanization in Shanghai, China. Weed Biology and Management 15 (1), 27–41. https://doi.org/10.1111/wbm.12062.

Tian, L., Yin, S., Ma, Y.G., Kang, H.Z., Zhang, X.Y., Tan, H.X., Liu, C.J., 2019. Impact factor assessment of the uptake and accumulation of polycyclic aromatic hydrocarbons by plant leaves: morphological characteristics have the greatest impact. Sci. Total Environ. 652, 1149–1155. https://doi.org/10.1016/j.scitotenv.2018.10.357.

Tobiszewski, M., Namiesnik, J., 2012. PAH diagnostic ratios for the identification of pollution emission sources. Environ. Pollut. 162, 110–119. https://doi.org/10.1016/j.envpol.2011.10.025.

United States Environmental Protection Agency, 2014. Priority pollutant list. https://www.epa.gov/sites/production/files/2015-09/documents/priority-pollutant-list-epa.pdf, Accessed date: 30 September 2019.

Wang, W.T., Simonich, S.L.M., Xue, M.A., Zhao, J.Y., Zhang, N., Wang, R., ... Tao, S., 2010. Concentrations, sources and spatial distribution of polycyclic aromatic hydrocarbons in soils from Beijing, Tianjin and surrounding areas, North China. Environmental Pollution 158 (5), 1245–1251. https://doi.org/10.1016/j.envpol.2010.01.021.

Wang, H.B., Qin, J., Bin, Z., Chen, J.K., Dong, L., Hu, Y.H., 2017. Spatiotemporal dynamics of plant diversity in response to farmers' evolved settlements in Shanghai. Urban For. Urban Green. 22, 64–73. https://doi.org/10.1016/j.ufug.2017.04.006.

Wang, W.J., Zhang, B., Zhou, W., Lv, H.L., Xiao, L., Wang, H.Y., ... He, X.Y., 2019b. The effect of urbanization gradients and forest types on microclimatic regulation by trees, in association with climate, tree sizes and species compositions in Harbin city, northeastern China. Urban Ecosystems 22 (2), 367–384. https://doi.org/10.1007/s11252-019-0823-9.

Xiao, Y.-h., Xi, D., Tong, F.-c., Kuang, Y.-w., Li, J., Chen, B.-f., ... Pan, Y.-j. (2013). Characteristics of rain season atmospheric PM2.5 concentration and its water-soluble ions contents in forest parks along an urban-rural gradient in Guangzhou City of South China. Chin. J. Appl. Ecol., 24(10), 2905–2911.

Yang, B., Liu, S., Liu, Y., Li, X.F., Lin, X.B., Liu, M., Liu, X., 2017. PAHs uptake and translocation in Cinnamomum camphora leaves from Shanghai, China. Sci. Total Environ. 574, 358–368. https://doi.org/10.1016/j.scitotenv.2016.09.058.

Yu, Y., Yang, Y., Wang, Q., Liu, M., 2018. Distribution, sources, and risk assessment of PAHs in organic films on glass window surfaces along the urban–rural gradient in Shanghai, China. Polycycl. Aromat. Compd., 1–10 https://doi.org/10.1080/10406638.2018.1441880.

Yu, H.Y., Li, T.J., Liu, Y., Ma, LM., 2019. Spatial distribution of polycyclic aromatic hydrocarbon contamination in urban soil of China. Chemosphere 230, 498–509. https://doi.org/10.1016/j.chemosphere.2019.05.006.

Zhang, J.M., Yang, L.X., Ledoux, F., Courcot, D., Mellouki, A., Gao, Y., ... Wang, W.X., 2019. PM2.5-bound polycyclic aromatic hydrocarbons (PAHs) and nitrated PAHs (NPAHs) in rural and suburban areas in Shandong and Henan Provinces during the 2016 Chinese New Year's holiday. Environmental Pollution 250, 782–791. https://doi.org/10.1016/j.envpol.2019.04.040.

Zhao, X.L., Zhou, W.Q., Han, L.J., 2019. Human activities and urban air pollution in Chinese mega city: an insight of ozone weekend effect in Beijing. Phys. Chem. Earth 110, 109–116. https://doi.org/10.1016/j.pce.2018.11.005.